

A Mathematical Model for the Drying Characteristics of Microalgae (*Tetraselmis sp.*)

Alvin B. Culaba^{1,4*}, Raymond R. Tan^{2,4}, Jose Bienvenido Manuel M. Biona^{1,4}, Aristotle T. Ubando^{1,4}, Neil Stephen A. Lopez^{1,4}, Joel Q. Tanchuco³, Soledad S. Garibay⁵, Nieves A. Toledo⁵, Caridad N. Jimenez⁵, Ida G. Pahila⁵ and Letty S. Ami⁵

¹Mechanical Engineering Department, De La Salle University, Philippines

²Chemical Engineering Department, De La Salle University, Philippines

³School of Economics, De La Salle University, Philippines

⁴Center for Engineering and Sustainable Development Research (CESDR), De La Salle University, Philippines

⁵Institute of Aquaculture, College of Fisheries and Ocean Sciences/Division of Chemistry, College of Arts and Sciences, University of the Philippines – Visayas, Philippines

Microalgae are some of the most promising sources of biofuel, but their high initial moisture content remains a hindrance to efficient lipid extraction. A major concern that affects the economic feasibility of microalgal biofuel is the drying process. An experimental drying setup was used to analyze the drying characteristics of *Tetraselmis sp.* The drying characteristic of the microalgae was assessed through radiation heat intensity, air flow velocity, and

convective heat input employing a Taguchi orthogonal array design of experiments. The analysis of variance resulted in a linear regression model relating the effects of the three factors mentioned with the three responses: average chamber temperature, average microalgae slurry surface temperature, and average drying rate. The study developed a mathematical model fitted in Newton's drying kinetics model. The results showed the effect of varying the values of the three factors, reflected in the drying coefficient k of the derived mathematical model.

KEYWORD

Newton's drying model, Taguchi orthogonal array, Microalgae, *Tetraselmis sp.*, Drying characteristics

INTRODUCTION

The rising concern about global warming and the increasing price of petroleum are now being taken seriously, so that biofuels are considered an alternative replacement for fossil fuels (Patil et al. 2008, Christi 2007). Biofuels are advanced

*Corresponding author

Email Address: alvin.culaba@dlsu.edu.ph

Submitted: December 3, 2012

Revised: April 17, 2013; July 10, 2013

Accepted: July 11, 2013

Published: November 22, 2013

Editor-in-charge: Eduardo A. Padlan

fuels which are primarily derived from biomass. However, conventional biomass feedstock available for biofuel production poses social, environmental, and agricultural threats as it competes with the land requirements of food crops. Among the advanced biomass feedstock, which show potential for biofuel production, are microalgae. Microalgae are unicellular bioorganisms that convert carbon dioxide into usable applications such as algal feeds, high-value nutraceuticals, and biofuels. Their high photosynthetic efficiency (Huntley and Redalje 2007) compared to other crops makes them a viable option for an efficient conversion of solar energy to biomass feedstock. A comparison of biofuel feedstock showed promising results for microalgae biofuel production, which has the highest oil yield per land area while not compromising the production of food and other products derived from crops (Christi 2007). Biofuel production from microalgae can be broken down into four major processes: 1) cultivation, 2) harvesting, 3) lipid extraction, and 4) biofuel production by transesterification (Khoo et al. 2011). The large initial moisture content of microalgae causes problems during the oil extraction. Microalgal biomass has an initial moisture content of 80-90%, wet-basis. Even after free water had already been removed from harvesting, further dehydration of

microalgal biomass is still necessary for efficient oil extraction. The centrifugation and the drying process accounts for about 25-30% of the total cost of cultivation and harvesting, as well as a similar proportion of total energy demand (Prakash et al. 1997). According to Halim et al. (2011), the lipid yield of dried microalgae is 33% higher than that of wet microalgae using hexane extraction. On the other hand, mechanical oil extraction processes are only possible at moisture content levels of at most 10% (Becker 1994, Prakash et al. 1997, Show et al. 2013). The utilization of a solar dryer would significantly reduce the cost of microalgal biofuel production and the energy requirement.

In the Philippines, the Congressional Commission on Science and Technology and Engineering (COMSTE), the Commission on Higher Education (CHED), the Department of Agriculture (DA), and the Department of Science and Technology (DOST) are currently working together to develop the Philippine Algae Research Center (PARC) (SP 2011). PARC envisions increasing the research on microalgae cultivation and developing processes to produce microalgal products such as pharmaceuticals, animal feeds, and biofuels. Since the Philippines is a tropical country, it is ideal to use solar dryers in processing biomass products.



Figure 1. Algal starters of *Tetraselmis* sp. in 1-liter, 5-liter, and 18-liter containers.



Figure 2. *Tetraselmis* culture in 1-ton capacity fiberglass tanks and 25-T canvass-lined ponds.

Solar dryers have long been developed for drying various types of agricultural crops. A solar dryer is composed of two major parts: the solar air heater and the drying chamber. The former serves as the air collector of the dryer; it is where heated air enters the dryer. The latter is placed in the drying chamber for the dehumidifying process. Extensive literature reviews of solar drying types for various applications have been reported by Jairaj et al. (2009) and Fudholi et al. (2010). Bennamoun (2011) described the three modes of solar dryers as direct, indirect, and mixed. Direct mode solar dryers, also known as integral mode solar dryers, employ glazing which allows direct solar radiation. Indirect mode solar dryers, also known as distributed mode solar dryers, use absorber plates which absorb heat from the sun. A mixed mode solar dryer uses both an indirect mode dryer as a solar air collector and a direct mode dryer for the drying chamber. Solar dryers are of two major types: active or forced convection type,

and passive or natural convection type. Active types of dryers employ fans, either found in the inlet or outlet, for forced flow of air in the drying chamber. A matrix composed of 6 combinations of the different modes and types of the solar dryer can be generated. Simate (2003) reported his work on minimizing the cost of mixed-mode and indirect-mode solar dryers for chilli. Banout et al. (2011) evaluated the performance of a double-pass solar dryer for red chilli on the basis of the drying efficiency together with drying costs. Forson et al. (2007a) made an analysis of a laboratory-scale mixed mode solar dryer for cassava, utilizing the diffusion equation for a slab-shaped bed. Gbaha et al. (2007) used a direct solar dryer to dry banana, cassava, and mango, while evaluating the influence of drying parameters, such as solar incident radiation, drying air mass flow, and thermal performance. Forson et al. (2007b) outlined a systematic methodology for designing a solar dryer based on best known methods from previous experimental studies.

Drying is a very energy-intensive process, making the option to use free energy of the sun very attractive. Prakash et al. (1997) published a report on using a mixed-mode solar dryer to dry two microalgae – *Spirulina* and *Scenedesmus*. Meanwhile, Viswanathan et al. (2011) reported the drying characteristics of a consortium of microalgae composed of *Scenedesmus bijuga*, *Chlamydomonas globosa*, and *Chlorella minutissima*, utilizing 3 models of drying characteristics, namely, the Henderson and Pabis model, the Newton model, and the Page model.

The present study aims to develop a mathematical model of the drying characteristics of *Tetraselmis sp.* using a fabricated dryer, varying the solar radiation intensity, the air flow velocity, and the convective heat input. The data generated by this study will aid future researchers in developing better solar drying systems and analyzing their potential.

The paper is organized as follows. The next section provides information on the materials and methods used in this study. Then, the results of the experiment and its discussion is tackled next. Lastly, a summary of the study is discussed together with its possible future work.

MATERIALS AND METHODS

This section discusses the materials utilized and the methodology employed in the study. It is subdivided into four parts: microalgae cultivation, design of experiment for drying, dryer experimental setup, and mathematical modeling of drying curves.

Microalgae cultivation

The microalgae cultivation stage was conducted at the University of the Philippines Visayas (UPV) after which the microalgal cake was transferred to De La Salle University (DLSU) Manila for drying. This section discusses the culture protocol and the harvest method of *Tetraselmis sp.* in UPV.

Culture protocol. A unialgal culture of *Tetraselmis sp.* was maintained at the hatchery laboratory of the Institute of Aquaculture, College of Fisheries and Ocean Sciences, UPV. The culture followed the current practice in aquaculture, which is the batch and sustenance culture method. It was started from a single inoculation of cells in a container of fertilized seawater, followed by a growing period of 3 to 5 days, and finally harvesting when the algal population reached its peak density for culture in 1 liter.

Ten to thirty per cent of the pure algae were transferred to a 1-liter sterile dextrose bottle containing sterile seawater. The culture was fertilized with TMRL enrichment medium composed

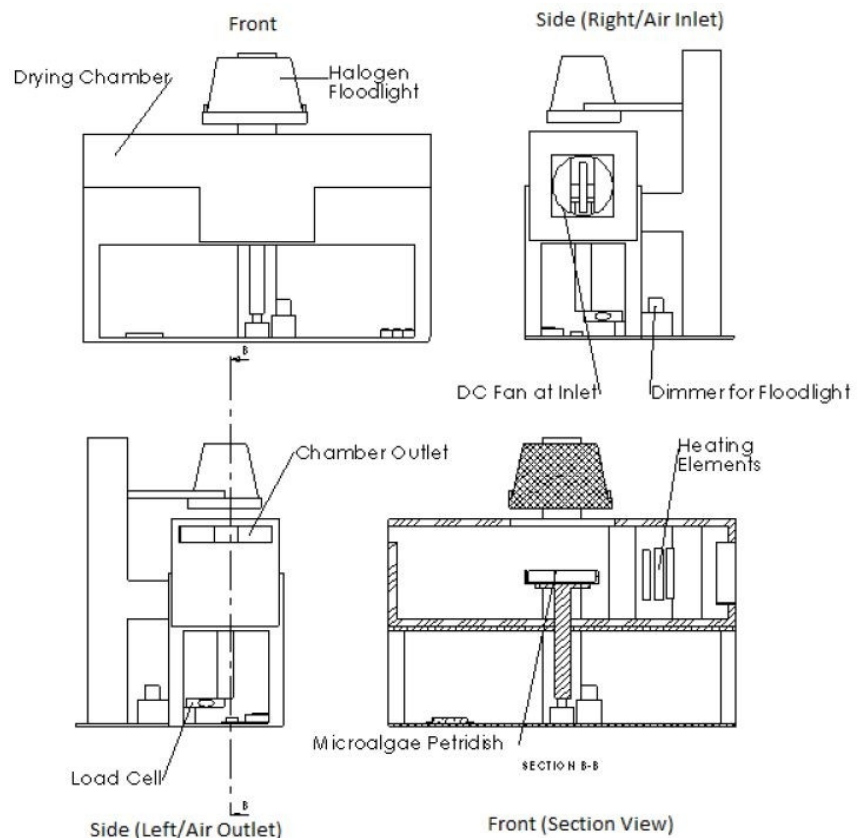


Figure 3. Schematic diagram of the experimental setup. Dimensions of the drying chamber: 120mm × 120mm × 450mm; Air outlet cross-section: 120mm × 20mm; Air inlet diameter: 80 mm with DC voltage controlled fan; Petri dish diameter: 100 mm. Specifications: Heating elements: 3 × 40 W; Halogen flood light, 150W, dimmer controlled; Load Cell – 1 kg max, 0.1 g sensitivity.

of KNO_3 , $\text{Na}_2\text{HPO}_4 \cdot 12\text{H}_2\text{O}$, and $\text{FeCl}_3 \cdot 6\text{H}_2\text{O}$ at 1 mL per liter application. Culture water was then provided with aeration to ensure even distribution of the *Tetraselmis* cells. The alga was cultured in 24-hr light for 3 to 5 days until it reached the logarithmic phase. The 1-liter culture was then scaled up indoors to 10-L plastic carboys and 18-liter containers, at 18-24°C and pH 7-9. Figure 1 shows the algal starters of *Tetraselmis sp.*

From the indoor culture, *Tetraselmis sp.* was transferred

outdoors into 250-liter fiberglass tanks. At its logarithmic phase, the algae were then scaled up to 1-ton, then 10-ton canvass-lined tanks, and, finally, to 25-ton canvass-lined ponds with aeration. The seawater used for culture was filtered using 0.2-1.0 μm filter bags prior to use and fertilized using technical grade commercial fertilizers (ammonium sulphate, mono-ammonium phosphate, and urea at a ratio of 2:1:1), as shown in Figure 2. The alga was cultured under ambient temperature, salinity, and photoperiod.

The density of the alga was monitored daily by counting the algal cells using a hemacytometer. Other water parameters were also regularly monitored. Water temperature was measured using a laboratory thermometer. Salinity, dissolved oxygen, pH, and light intensity were measured using a refractometer, DO meter, pH meter, and a wide-range Lux meter, respectively.

Harvest method. Harvest and collection of *Tetraselmis sp.* were facilitated by concentrating the cells through flocculation by chemical method. The concentrated cells were allowed to settle for 24 hours prior to separation. The concentrated cells were passed through filters and the cells collected in paste or cake form. The microalgal cake was then shipped to DLSU for the drying experiment.

Design of experiments for drying

One of the objectives of the study is to see the effects of the direct radiation, air velocity, and heat input to the resulting average chamber temperature (T_{ch}), average surface temperature of the microalgal slurry (T_s), and the average drying rate (DR_{ave}). A design-of-experiment approach employing a Taguchi orthogonal array (TAO) (Montgomery and Runger 2003) is used to evaluate a three-level three-factor design resulting in nine orthogonal-array experiments as seen in Table 1. The Design Expert 6 software package is utilized in the analysis of the results of the TAO. The three direct radiation values considered for the study are 0 W/m^2 , 280 W/m^2 , and 490 W/m^2 . The three air velocity values considered are 1.3 m/s, 1.9 m/s,

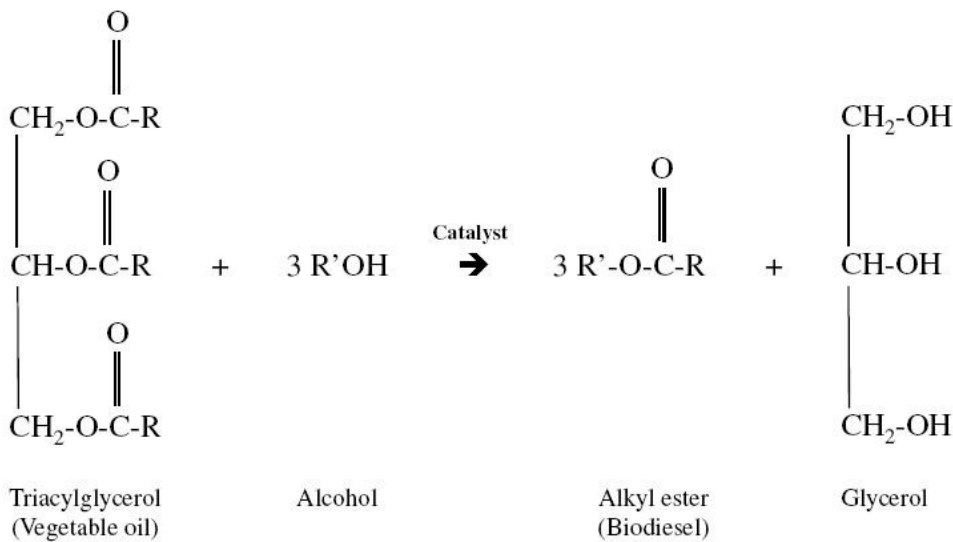


Figure 4. Transesterification reaction to produce biodiesel from triacylglycerol (Knothe et al., 2005).

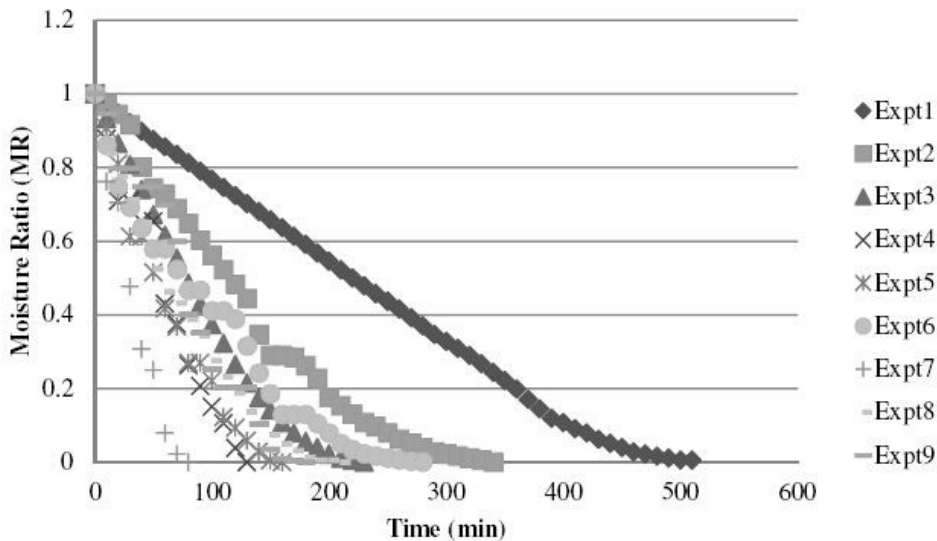


Figure 5. Actual results of the experimental data: moisture content versus time plot.

and 2.2 m/s. Lastly, the three heat inputs considered in the drying chamber are 40 W, 80 W, and 120 W.

In Design Expert, using a two-factor interaction, the effects of the factors to each response is evaluated using the analysis of variance (ANOVA). The ANOVA results are fitted to the 2-factor interaction formula using a linear regression of the form:

$$Y_i = \beta_0 + \beta_1 X_1 + \beta_2 X_2 + \beta_3 X_3 + \beta_4 X_1 X_2 + \beta_5 X_1 X_3 + \beta_6 X_2 X_3 \quad (1)$$

where Y_i ($i = 1, 2,$ and 3) are the three responses: the average chamber temperature T_{ch} , the average microalgae slurry surface temperature T_s , and the average drying rate DR_{ave} ; $X_1, X_2,$ and X_3 are the three factors: direct radiation (Q_r), air velocity (V_f), and heat input (Q_c), respectively; β_0 is the regression intercept; $\beta_1, \beta_2,$ and β_3 are the main factor coefficients; $\beta_4, \beta_5,$ and β_6 are the two-factor interaction coefficients.

Replacing the three factors $X_1, X_2,$ and X_3 with each corresponding parameters: direct radiation (Q_r), air velocity (V_f), and heat input (Q_c), Equation (1) is rewritten as:

$$Y_i = \beta_0 + \beta_1 Q_r + \beta_2 V_f + \beta_3 Q_c + \beta_4 Q_r V_f + \beta_5 Q_r Q_c + \beta_6 V_f Q_c \quad (2)$$

The parameter Y_i ($i = 1, 2,$ and 3) can be replaced with the individual response parameters: average chamber temperature (T_{ch}), average surface temperature of the microalgae slurry (T_s), and the average drying rate (DR_{ave}), correspondingly. Equation (2) can be expressed in the following equations:

$$T_{ch} = \beta_0 + \beta_1 Q_r + \beta_2 V_f + \beta_3 Q_c + \beta_4 Q_r V_f + \beta_5 Q_r Q_c + \beta_6 V_f Q_c \quad (3)$$

$$T_s = \beta_0 + \beta_1 Q_r + \beta_2 V_f + \beta_3 Q_c + \beta_4 Q_r V_f + \beta_5 Q_r Q_c + \beta_6 V_f Q_c \quad (4)$$

$$DR_{ave} = \beta_0 + \beta_1 Q_r + \beta_2 V_f + \beta_3 Q_c + \beta_4 Q_r V_f + \beta_5 Q_r Q_c + \beta_6 V_f Q_c \quad (5)$$

The accuracy of the curve fitting is evaluated using the coefficient of determination (r^2) for each response. The range of values for the coefficient of determination are $0 \leq r^2 \leq 1$, where 1 signifies that the model accounts for all of the variability of data and 0 denotes the failure of the model to account for any variability.

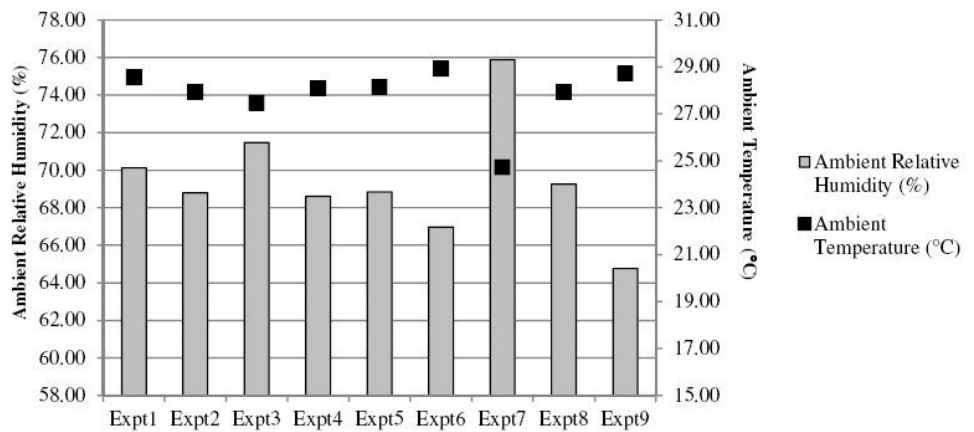


Figure 6. The average ambient relative humidity and average ambient temperature of the experiments.

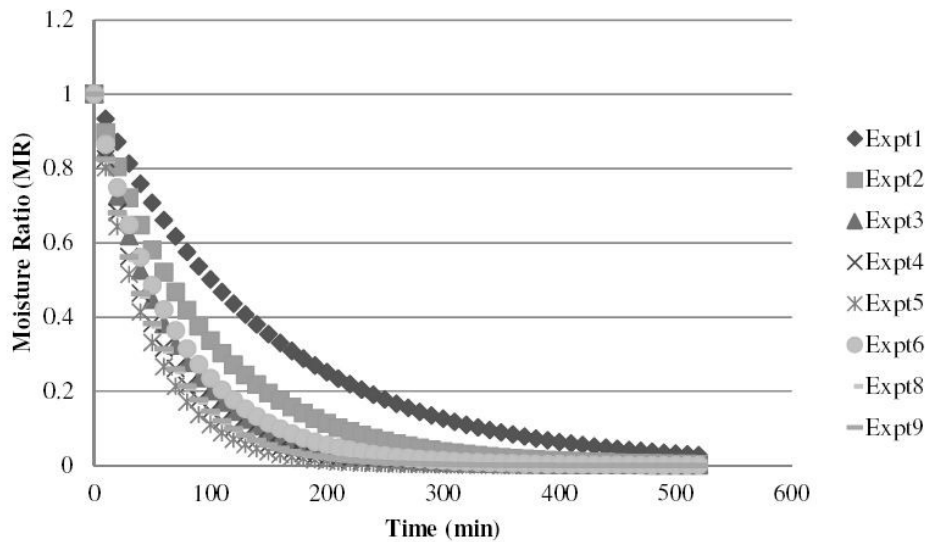


Figure 7. Results of curve fitting in Newton's solar drying kinetic model: moisture content versus time plot.

Drying experimental setup

The solar dryer experimental setup was designed and fabricated specifically to be able to vary the three factors of

drying, which are the direct solar radiation, the air velocity, and the heat input. The schematic diagram of the fabricated solar dryer is seen in Figure 3. The drying chamber has a cross-section of 120mm × 120mm and a length of 450mm. The sides of the drying chamber are covered with an insulating material to represent an adiabatic wall. In Figure 3, a halogen flood light is utilized as a source of direct radiation whose intensity is controlled through a dimmer and measured by a solar pyranometer. The halogen light is located outside the drying chamber to eliminate any convective heat coming from the lamp, but is positioned just on top of the microalgae for them to receive only direct radiation. To employ varying air flow velocity inside the drying chamber, an 80mm-diameter fan is used together with a DC voltage-controller to regulate the air speed. The fan is positioned at the inlet of the drying chamber. A digital anemometer is deployed to measure the air velocity inside the drying chamber. To provide convective heat in the drying chamber, a three-cylindrical 40W heating element is installed between the fan and the microalgae. To achieve the varying values of heat input in the drying chamber identified in the design of the experiment, some of the heating elements are turned on or off. An air outlet is provided at the other end of the drying chamber to allow the moist air to exit the drying chamber. A petri dish is utilized to hold the microalgae inside the drying chamber. The instantaneous mass of the microalgae, plus the mass of the petri dish, is measured using a digital load cell having a resolution of 0.1 g. The measurement frequency of the instantaneous mass of the microalgae is 10 minutes. The average initial moisture content of the *Tetraselmis sp.* in the nine experiments was 0.894, each having a thin layer thickness of 4 mm. The chamber temperature and the microalgae surface temperature are measured using a conventional mercury thermometer and a laser thermometer, respectively. A digital hygrometer is used to measure the relative humidity of each experiment. All experiments were conducted until

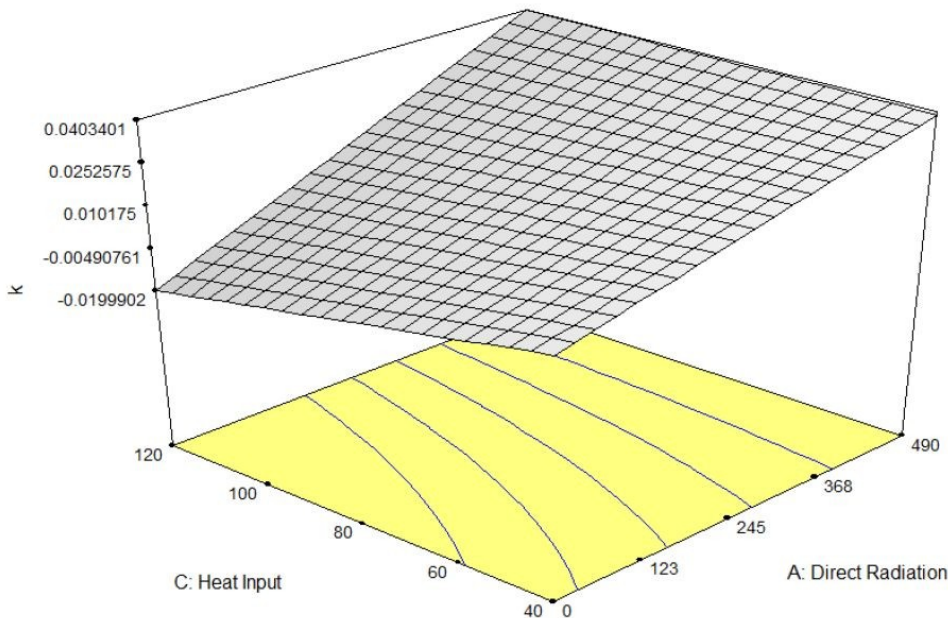


Figure 8. The drying coefficient k profile for air velocity of 1.3 m/s at varying direct radiation and convective heat input.

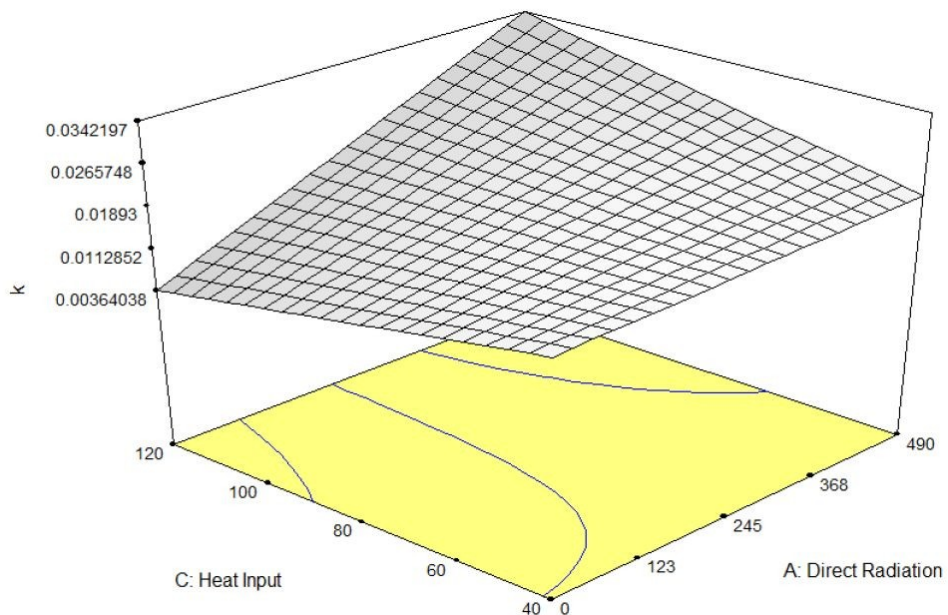


Figure 9. The drying coefficient k profile for air velocity of 1.9 m/s at varying direct radiation and convective heat input.

the desired moisture content of less than 10% is achieved.

model can be expressed similarly from Equation (7) as:

$$MR = e^{-kt} \tag{8}$$

The average drying rate (DR_{ave}) is calculated in terms of the mass of evaporated moisture per unit time (kg/min):

$$DR_{ave} = \frac{M_i - M_f}{t} \tag{6}$$

Where M_i and M_f are the initial and final moisture content and t is the time of drying.

The drying rate curve is composed of two stages: the constant rate (DR_c) and the falling rate (DR_f). The first stage is the constant rate during which the drying subject experiences constant drying characteristics while the exposed surface of the subject is still wet. When the surface of the subject starts to dry, additional energy is required to penetrate the subject letting the moisture creep out to the surface, giving rise to the falling rate stage.

Mathematical modeling of drying curves

Different mathematical models were used to fit the solar drying characteristics of various drying subjects as shown in Table 2. These models used are based on the fundamental nature of the drying curve which follows an exponential trend as shown in the equation (Weller and Bunn 1993, Bahnasawy and Shenana 2004):

$$MR = \frac{M - M_e}{M_i - M_e} = e^{-kt} \tag{7}$$

where MR is the moisture ratio, M_e is the equilibrium moisture content (dry basis), M_i is the initial moisture content (dry basis), M is the moisture content at time t , k is a drying constant, and t is the drying time (min).

The thin-layer Newton's drying

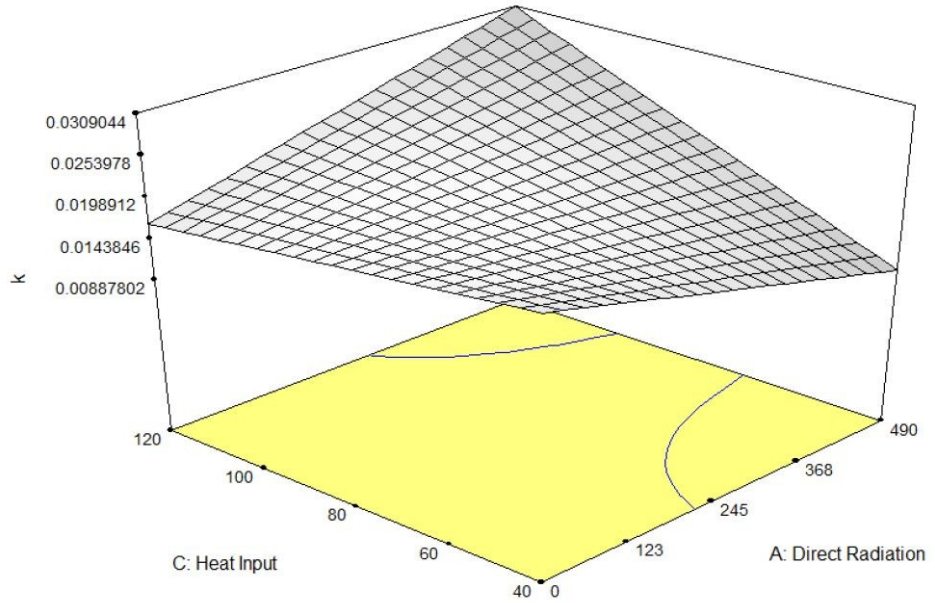


Figure 10. The drying coefficient k profile for air velocity of 2.2 m/s at varying direct radiation and convective heat input.

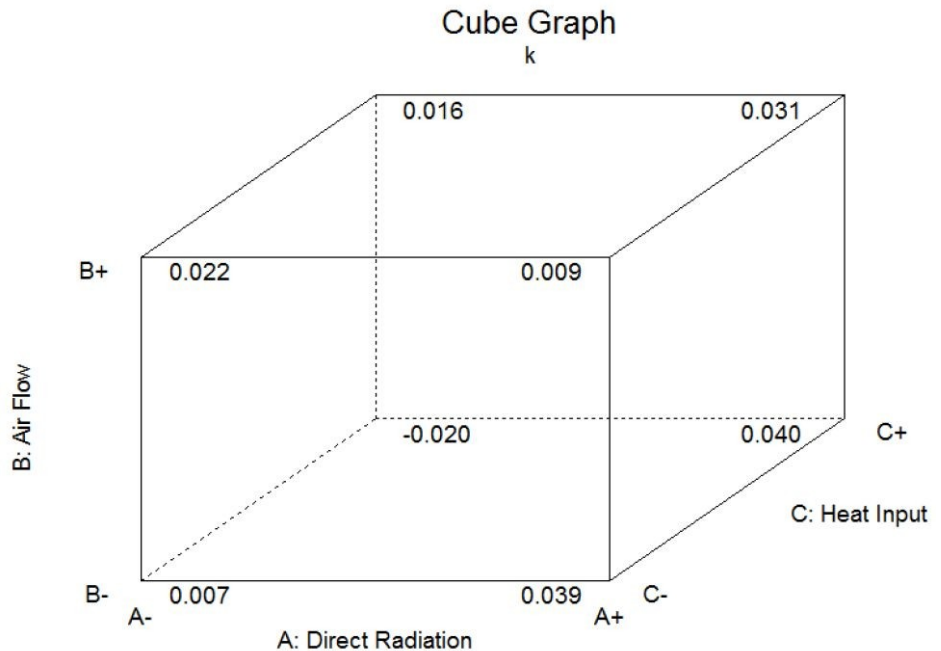


Figure 11. The cube graph of the drying coefficient k for the three factors: direct radiation, air velocity, and convective heat input.

To express Equation (8) in linear form, the natural logarithm of both sides is taken, and the equation can be rewritten as:

$$\ln(MR) = -kt \quad (9)$$

Table 1. The design of experiments using a Taguchi orthogonal array having 3 factors with 3 levels.

Taguchi: 3 factors with 3 levels			
Expt. No.	Direct Radiation (W/m ²)	Air Flow Rate (m/s)	Heat Input (W)
1	0	1.3	40
2	0	1.9	80
3	0	2.2	120
4	280	1.3	80
5	280	1.9	120
6	280	2.2	40
7	490	1.3	120
8	490	1.9	40
9	490	2.2	80

where $\ln(MR)$ denotes y , $-k$ is taken as the slope m , t represents x , and b is equal to zero in the linear equation $y = mx + b$. Applying linear regression on Equation (9), the value of k is then calculated based on the results of the experiment.

Further, the drying rate can be derived from Equation (7) by isolating M :

$$M = (M_i - M_e) e^{-kt} + M_e \quad (10)$$

Then, getting the first derivative of both sides with respect to time t leads to:

$$\frac{d}{dt} [M = (M_i - M_e) e^{-kt} + M_e] \frac{d}{dt} \quad (11)$$

$$\frac{dM}{dt} = - (M_i - M_e) k e^{-kt} \quad (12)$$

Equation (12) describes the rate of drying with respect to time using Newton's kinetic drying model.

The value of k is characterized by the moisture ratio MR as a function of the drying time t for the nine experiments. The k -value can also be expressed in the form of Equation (2) as:

Table 2. Various mathematical models for kinetics of solar drying (adapted from Dissa et al., 2011).

#	Name of Model	Equation	References
1	Newton	$MR = \exp(-kt)$	El-Sebaei et al. (2002)
2	Henderson and Pabis	$MR = a \exp(-bt)$	Mahmutoglu et al. (1996)
3	Page	$MR = \exp(-kt^y)$	Koua et al. (2009)
4	Modified Page	$MR = \exp(-(kt)^y)$	Togrul and Pehlivan (2002)
5	Logarithmic	$MR = a \exp(-kt) + c$	Yaldiz et al. (2001)
6	Two-term model	$MR = a \exp(-k_0t) + b \exp(-k_1t)$	Lahsasni et al. (2004)
7	Two-term exponential	$MR = a \exp(-k_0t) + (1 - a) \exp(-k_0at)$	Midilli and Kucuk (2003)
8	Verma et al.	$MR = a \exp(-k_0t) + (1 - a) \exp(-gt)$	Doymaz (2005)
9	Approximation of diffusion	$MR = a \exp(-k_0t) + (1 - a) \exp(-k_0bt)$	Usub et al. (2010)
10	Wang and Singh	$MR = 1 + at + bt^2$	Koua et al. (2009)

$$k = \beta_0 + \beta_1 Q_r + \beta_2 V_f + \beta_3 Q_c + \beta_4 Q_r V_f + \beta_5 Q_r Q_c + \beta_6 V_f Q_c \quad (13)$$

Viswanathan et al. (2011) utilized the Henderson and Pabis model, the Newton model, and the Page model to evaluate the consortium of microalgae with a cell count of 40%, 35%, and 25% for *Scenedesmus bijuga*, *Chlamydomonas globosa*, and *Chlorella minutissima*, respectively. Using the Newton's model, Viswanathan et al. (2011) calculated a range of k -values from 0.0005 to 0.004 for varying temperatures (30°C to 90°C) with a constant air flow velocity of 0.3 m/s in a convective oven.

The present study differs from that of Viswanathan et al. (2011) as it takes into consideration the effects of varying air flow velocity with varying heat input in the calculation of the k -values in Newton's model shown in Equation (8). This study evaluates the k -value profiles of the drying characteristics of *Tetraselmis sp.* using Newton's model through the three factors: direct radiation, air flow velocity, and heat input. The calculated k -values are then plotted based on the three-level three-factor results from the TOA design of experiments. The inclusion of varying solar radiation intensity in the solution of the k -values makes the methodology novel.

Quality of fatty acid methyl ester

The definition of biodiesel and its composition are from Chapter 1 of *The Biodiesel Handbook* (Knothe et al. 2005). Biodiesel is also known as fatty acid methyl ester (FAME), which is a biodegradable and nontoxic renewable energy source that has a lesser combustion emission profile (carbon dioxide, sulphur dioxide, and unburned hydrocarbon) compared to commercial diesel fuel. It is defined as a mono alkyl ester of long chain fatty acids derived from renewable lipid sources like plant and animal oils. The chemical range formula of biodiesel is C14-C24 methyl esters. To convert the dried microalgae to biodiesel, two process steps are required: oil extraction and transesterification. The oil extraction

is done through introduction of hexane as solvent. After extraction, the oil undergoes transesterification, during which alcohol is used to break the bond to the triacylglycerol to yield biodiesel. A co-product of biodiesel in the transesterification reaction is glycerol. Figure 4 shows the chemical reaction of the transesterification process.

Due to the limited resources of the study, a single sample of dried microalgae was processed for FAME using gas chromatography – mass spectrometry (GC-MS) at D&L Industries. The analysis assessed the quality of the dried microalgae with respect to the wet microalgae sample.

Table 3. Summary of the fitted model of the 9 experiments.

Expt. No.	Drying Coefficient, k	Newton's Model	r^2
1	0.00693	MR = exp(-0.00693t)	0.9147
2	0.01088	MR = exp(-0.01088t)	0.9431
3	0.01614	MR = exp(-0.01614t)	0.9256
4	0.01923	MR = exp(-0.01923t)	0.9358
5	0.02214	MR = exp(-0.02214t)	0.9034
6	0.01447	MR = exp(-0.01447t)	0.9434
7	0.04038	MR = exp(-0.04038t)	0.9207
8	0.01962	MR = exp(-0.01962t)	0.9353
9	0.01925	MR = exp(-0.01925t)	0.8480

Table 4. Comparison of simulated and actual chamber temperature T_{ch} .

Expt. No.	T_{ch} Equation (14)	Average of Actual T_{ch}	ΔT_{ch}	% difference
1	43.92	43.69	0.23	0.52%
2	44.75	44.88	0.13	0.30%
3	50.72	51.13	0.41	0.81%
4	57.54	58.50	0.96	1.65%
5	55.13	53.53	1.60	2.98%
6	36.16	36.07	0.09	0.26%
7	76.76	76.79	0.03	0.03%
8	41.97	41.14	0.82	2.00%
9	42.70	43.92	1.21	2.77%

Table 5. Comparison of simulated and actual microalgal slurry surface temperature T_s .

Expt. No.	T_s Equation (15)	Average of Actual T_s	ΔT_s	% difference
1	38.95	38.90	0.05	0.12%
2	40.40	38.60	1.80	4.67%
3	45.84	46.54	0.70	1.50%
4	50.42	52.05	1.63	3.12%
5	49.88	49.55	0.33	0.67%
6	36.35	37.75	1.40	3.71%
7	66.03	65.63	0.41	0.62%
8	41.54	40.15	1.39	3.46%
9	42.61	42.87	0.25	0.59%

Table 6. Comparison of simulated and actual average drying rate DR_{ave} .

Expt. No.	Simulated DR_{ave} Equation (16)	Actual DR_{ave} Equation (6)	ΔDR_{ave}	% difference
1	0.03498	0.03451	0.00047	1.37%
2	0.05822	0.05333	0.00488	9.15%
3	0.07296	0.08045	0.00749	9.31%
4	0.12858	0.13769	0.00911	6.62%
5	0.13487	0.12750	0.00737	5.78%
6	0.05917	0.06357	0.00441	6.93%
7	0.25238	0.25143	0.00095	0.38%
8	0.08407	0.08000	0.00407	5.09%
9	0.10676	0.11222	0.00546	4.86%

Table 7. Comparison of GC-MS results of dried microalgae and wet microalgae.

FAME Composition (%)	Dried Microalgae	Wet Microalgae
C6 (Caproic Acid)	9.38	36.34
C10 (Capric Acid)	3.69	0
C12 (Lauric Acid)	3.18	0
C16 (Palmitic Acid)	3.15	0
C18:0C (Stearic Acid)	0	0
C18:1C (Oleic Acid)	1.66	0
C18:2C (Linoleic Acid)	1.62	0
C18:3C (alpha-Linolenic Acid)	1.94	0
C20:1 (Eicosenoic Acid)	0	36.52
OFA (Other Fatty Acid)	75.38	27.14
Total	100	100

RESULTS AND DISCUSSION

This section discusses the results of the experiments and elaborates the details of the effects of the three factors with the responses. Further, the result of fitting the drying curve into Newton's mathematical model is presented.

Solar drying experimental results

The results of the nine experiments yielded the moisture content versus time curves shown in Figure 5. As shown in Figure 4, the longest drying time was Experiment 1, followed by Experiment 2. The least drying time required was Experiment 7. The ambient relative humidity and the ambient temperature for all the experiments are presented in Figure 6. It is interesting to note that even when the ambient relative humidity was high at 75.89% and the ambient temperature was low at 24.73 °C in Experiment 7, the result was the least drying time. This was due to the fact that the irradiance was high, the air velocity was low, and convective heat was high. The significance of the effects of the factors to each response can be analyzed through the *p-value*. If the *p-value* is less than the level of significance of $\alpha = 0.05$, the factor is significantly affecting the response. For all the three responses, namely, average chamber temperature (T_{ch}), average surface temperature of the microalgae slurry (T_s), and the average drying rate (DR_{ave}), there were no specific significant effects due to each of the factors where the two-factor interactions have had *p-values* greater than 0.05. However, the complete model terms showed a significant effect on the three responses (T_{ch} , T_s , and DR_{ave}) with *p-values* of 0.0149, 0.0481, and 0.027, respectively. The linear regression model for the three responses yielded the following relations:

$$\begin{aligned}
 T_{ch} = & 59.678063 + 0.139336 Q_f - \\
 & 7.937558 V_f - 0.434831 Q_c - \\
 & 0.087381 Q_f V_f + 0.000529 Q_f Q_c + \\
 & 0.229854 V_f Q_c \quad (14)
 \end{aligned}$$

$$\begin{aligned}
T_s = & 50.92072 + 0.11685 Q_r - 5.05406 V_f \\
& - 0.40286 Q_c - 0.069734 Q_r V_f + 0.000426 Q_r Q_c \\
& + 0.206 V_f Q_c
\end{aligned} \tag{15}$$

$$\begin{aligned}
DR_{ave} = & - 0.005344 + 0.000521 Q_r \\
& + 0.033697 V_f - 0.000263 Q_c \\
& - 0.000305 Q_r V_f + 0.0000028 Q_r Q_c \\
& + 0.000135 V_f Q_c
\end{aligned} \tag{16}$$

The coefficients of determination r^2 of Equations (14-16) are 0.995, 0.984, and 0.991, respectively.

The linear regression models developed can be used to predict the average chamber temperature (T_{ch}), the average surface temperature of the microalgae slurry (T_s), and the average drying rate (DR_{ave}) with varying values of the direct radiation from 0 W/m² to 490 W/m², the air flow velocity from 1.3 m/s to 2.2 m/s, and the heat input of 40 W to 120 W; limited to a thin layer microalgae slurry of 4mm.

Fitting of drying curve in newton's model

Using Newton's solar drying kinetic model, the results of the experimental data are fitted using Equation (9) and then reverted back to the form of Equation (8) to produce the moisture ratio versus time graph shown in Figure 7. The quantification of the drying coefficient k for each experiment and the fitted model into Newton's model for each experiment is shown in Table 3. In Table 3, the resulting Newton's model for each experiment and the coefficients of determination r^2 for each experiment are also exhibited. The highest value of r^2 for the fitted model were seen in Experiment 6 followed by Experiment 2 with values of 0.9434 and 0.9431, respectively. The ANOVA result for the drying constant k showed significant effects from direct radiation Q_r , interaction of direct radiation and air velocity $Q_r V_f$, and interaction of direct radiation and heat input $Q_r Q_c$, with p -values of 0.0117, 0.0272, and 0.0415, respectively. This means that the drying coefficient k is highly sensitive to the interaction of direct radiation and heat input $Q_r Q_c$, followed by the interaction of direct radiation and heat input $Q_r Q_c$, then lastly, the effect of direct radiation Q_r . The complete linear regression model also showed significance with a p -value of 0.009. The resulting linear regression model for the drying coefficient k is:

$$\begin{aligned}
k = & 0.013063 + 0.000173 Q_r + 0.005497 V_f \\
& - 0.000714 Q_c - 0.000104 Q_r V_f \\
& + 0.00000071 Q_r Q_c + 0.000292 V_f Q_c
\end{aligned} \tag{17}$$

The coefficient of determination r^2 for the linear regression model for the drying coefficient k is 0.997. The surface profiles of the drying coefficient k at fixed air velocity V_f , with varying values of heat input Q_c and direct radiation Q_r , are shown in Figure 8 to Figure 10. The resulting cube graph of the drying coefficient k , with the three axes corresponding to the three factors, direct radiation Q_r , air velocity V_f , and heat input Q_c , is shown in Figure 11.

Nusselt number

The Nusselt number describes the convective heat transfer at the surface of the drying subject. It is characterized by the Reynolds number and the Prandtl number as given by (Holman 1997, Maloney 2008):

$$Nu = 0.644 Re^{1/2} Pr^{1/2} \tag{18}$$

Where Re is the Reynolds number and Pr is the Prandtl number. The Reynolds number and the Prandtl number are described by the following relations (Holman 1997, Maloney 2008):

$$Re = \frac{VL}{\nu} \tag{19}$$

$$Pr = \frac{C_p \mu}{k_{th}} = 0.7 \tag{20}$$

Where V is the velocity of air, L is the length of the surface slurry which is given at 0.225 m, ν is the kinematic viscosity of air, C_p is the specific heat of air, μ is the dynamic viscosity of air, and k_{th} is the thermal conductivity. The Reynolds number is a dimensionless value which describes the level of flow disturbance in terms of its velocity profile and is expressed as laminar or turbulent. The Prandtl number is also a dimensionless value which relates the hydrodynamic thickness with the thermal boundary layer. It is assumed that the Prandtl number for all experiments has a value of 0.7 (Holman 1997) with the following consideration: a constant surface temperature at a flat plate condition. Moreover, the velocity of the fan V_f , is assumed equal to the air velocity V , at the microalgae surface.

Substituting the expressions for Re and Pr in Equations (19) and (20) into Equation (18) and isolating the velocity V_f yields:

$$V_f = 14.4 \text{ Nu}^2 \nu \quad (21)$$

Relating the k -value as a function of Nusselt number, Equation (17) becomes:

$$k = 0.013063 + 0.000173 Q_r + 0.079161 \text{ Nu}^2 \nu - 0.000714 Q_c - 0.001498 Q_r \text{ Nu}^2 \nu + 0.00000071 Q_r Q_c + 0.004205 \text{ Nu}^2 \nu Q_c \quad (22)$$

By replacing the equivalent equation of fan velocity V_f in Equation (21) into Equation (17), Equation (22) now shows the relation of the k -value in terms of direct radiation Q_r , heat input Q_c , Nusselt number Nu , and the kinematic viscosity of air ν .

Mathematical model validation

The mathematical model validation compares the results of the three factors generated from the statistical relations shown in Equations (14) to (16) with the average actual readings of the experiments. The comparison of the chamber temperature T_{ch} , the microalgal slurry surface temperature T_s , and the average drying rate Dr_{ave} are presented in Tables 4 to 6, respectively. The actual chamber temperatures shown in Table 4 are the average chamber temperature readings for each experiment measured with a mercury thermometer. The actual microalgal slurry surface temperatures shown in Table 5 are the average surface temperature readings for each experiment measured with an infrared thermometer. In Table 6, the actual average drying rate values were computed using Equation (6). The percent differences of all the three responses shown in Tables 4 to 6 are less than 10% which signifies a strong predicting capability of the equations developed within the factor limits.

Quality of fatty acid methyl ester

The results of the GC-MS comparison of dried microalgae and wet microalgae are shown in Table 7. Since the chemical range formula of biodiesel is from C14 to C24 methyl esters, the results show that the dried microalgae have a complete range of biodiesel composition compared to wet microalgae. Since the sample of the experiment is limited to only 1 sample of dried microalgae and 1 sample of wet microalgae, a full study on the GC-MS of dried microalgae is recommended.

CONCLUSION

The developed mathematical model for the drying of microalgae *Tetraselmis sp.* evaluated the effects of the direct radiation, air flow velocity, and the convective heat input with respect to the average chamber temperature, average microalgal slurry surface temperature, and the drying rate using a Taguchi orthogonal array design of experiments. The Newton's solar drying kinetic model was used to fit the results of the

experimental data to characterize the value of the drying coefficient k . A linear regression model was developed to link the drying coefficient k with the effects of the three factors: direct radiation, air flow velocity, and the convective heat input. Furthermore, the drying coefficient k was also expressed as a function of the Nusselt number. The results can be used to design a solar dryer which can efficiently augment the energy requirements in the production of biodiesel from microalgae.

Future studies will involve the fitting of the experimental data with other solar drying kinetics models such as the Henderson and Pabis model and the Page model. The opportunity for validating the mathematical model developed using a laboratory scale solar dryer shall be pursued. A full GC-MS analysis of the esterified samples should be done in future microalgal drying studies.

NOMENCLATURE

Parameters

β_0	Linear regression intercept
β_1	Coefficient of the 1 st factor in the linear regression
β_2	Coefficient of the 2 nd factor in the linear regression
β_3	Coefficient of the 3 rd factor in the linear regression
β_4	Coefficient of the interaction of the 1 st and 2 nd factors in the linear regression
β_5	Coefficient of the interaction of the 1 st and 3 rd factors in the linear regression
β_6	Coefficient of the interaction of the 2 nd and 3 rd factors in the linear regression
dM/dt	Infinitesimal rate of drying with respect to time
M_i	Initial moisture content of microalgae slurry (g)
M_f	Final moisture content of microalgae slurry (g)
M_e	Equilibrium moisture content of microalgae slurry (g)
M	Instantaneous moisture of microalgae slurry (g)
MR	Moisture ratio
Nu	Nusselt number
Pr	Prandtl number
Re	Reynolds number
t	Time (min)
V	Velocity of air at the microalgae slurry
k_{th}	thermal conductivity
L	Length of the surface of the microalgae slurry
ρ	Density of air at the surface of microalgae slurry
μ	Dynamic viscosity of air at the surface of microalgae slurry
ν	Kinematic viscosity of air at the surface of microalgae slurry

Variables

Y_i	Dependent variable in the linear regression, representing the responses
X_1	First independent variable in the linear regression representing the 1 st factor
X_2	Second independent variable in the linear regression representing the 2 nd factor
X_3	Third independent variable in the linear regression representing the 3 rd factor
T_{ch}	Average chamber temperature ($^{\circ}\text{C}$), representing the 1 st response, Y_1
T_s	Average microalgal surface temperature ($^{\circ}\text{C}$), representing the 2 nd

response, Y_2
 DR_{ave} Average drying rate (g/min), representing the 3rd response, Y_3
 Q_r Direct radiation (W/m^2), representing the 1st factor, X_1
 V_f Air flow velocity (m/s), representing the 2nd factor, X_2
 Q_c Convective heat input (W), representing the 3rd factor, X_3
 k Drying coefficient
 p -value, α Level of significance in the ANOVA
 r^2 Coefficient of determination in the ANOVA

ACKNOWLEDGEMENT

The financial support of the Science Foundation and University Research Coordinating Office of De La Salle University is gratefully acknowledged.

CONFLICT OF INTEREST STATEMENT

This is a De La Salle University (DLSU)-funded research under the University Research Coordination Office with project number 10IRS 3 10. No government funding support for the research. Nature of collaboration with University of the Philippines Visayas is the supply and the analysis of the microalgae material. Collaborators from University of the Philippines Visayas focused mainly on scientific grounds.

CONTRIBUTION OF INDIVIDUAL AUTHORS

Alvin B. Culaba, De La Salle University, Principal investigator; energy analysis. Raymond R. Tan, De La Salle University, Co-investigator; energy systems modeling. Jose Bienvenido Manuel M. Biona, De La Salle University, Mathematical model development. Aristotle T. Ubando, De La Salle University, Mathematical model development. Neil Stephen A. Lopez, Sun Power Inc. (former DLSU graduate student), Graduate research student; design and fabrication of dryer. Joel Q. Tanchuco, De La Salle University, Economic analysis. Soledad S. Garibay University of the Philippines Visayas, Collaborator; Cultivation, harvesting, and analysis of microalgae material. Nieves A. Toledo, University of the Philippines Visayas, Collaborator; Cultivation, harvesting, and analysis of microalgae material. Caridad N. Jimenez, University of the Philippines Visayas, Collaborator; Cultivation, harvesting, and analysis of microalgae material. Ida G. Pahila, University of the Philippines Visayas, Collaborator; Cultivation, harvesting, and analysis of microalgae material. Letty S. Ami, University of the Philippines Visayas, Collaborator; Cultivation, harvesting, and analysis of microalgae material.

REFERENCES

Bahnasawy AH, Shenana ME. A mathematical model of direct sun and solar drying of some fermented dairy products (Kishk). *Journal of Food Engineering* 2004; 61:309-319.
 Banout J, Ehl P, Havlik J, Lojka B, Polensy Z., Verner V. Design and performance evaluation of a Double-pass solar drier for drying of red chilli (*Capsicum annum* L.). *Solar*

Energy 2011; 85:506-515.
 Becker EW. *Microalgae: Biotechnology and Microbiology*. In Carey NH, Higgins IJ, Potter WG (eds) Sir J Baddiley, Cambridge University Press: United Kingdom, 1994.
 Bennamoun L. Reviewing the experience of solar drying in Algeria with presentation of the different design aspects of solar dryers. *Renewable and Sustainable Energy Reviews* 2011; 15:3371-3379.
 Christi Y. Biodiesel from microalgae. *Biotechnology Advances* 2007; 25:294-306.
 Dissa AO, Bathiebo DJ, Desmorieux H, Coulibaly O, Koulidiati J. Experimental characterization and modelling of thin layer direct solar drying of Amelie and Brooks mangoes. *Energy* 2011; 36:2517-2527.
 Doymaz I. Sun drying of figs: an experimental study. *Journal of Food Engineering* 2005; 71:403-407.
 El-Sebaili AA, Aboul-Enein S, Ramadan MRI, El-Gohary HG. Empirical correlations for drying kinetics of some fruits and vegetables. *Energy* 2002; 27:845-859.
 Forson FK, Nazha MAA, Rajakaruna H. Modelling and experimental studies on a mixed-mode natural convection solar crop-dryer. *Solar Energy* 2007a; 81:346-357.
 Forson FK, Nazha MAA, Akufo FO, Rajakaruna H. Design of mixed-mode natural convection solar crop dryers: Application of principles and rules of thumb. *Renewable Energy* 2007b; 32:2306-2319.
 Fudholi A, Sopian K, Ruslan MH, Alghoul MA, Sulaiman MY. Review of solar dryers for agricultural and marine products. *Renewable and Sustainable Energy Reviews* 2010; 14:1-30.
 Gbaha P, Andoh HY, Saraka JK, Koua BK, Toure S. Experimental investigation of a solar dryer with natural convective heat flow. *Renewable Energy* 2007; 32:1817-1829.
 Halim R, Gladman B, Danquah MK, Webley PA. Oil extraction from microalgae for biodiesel production. *Bioresource Technology* 2011; 102:178-185.
 Holman JP. *Heat Transfer*. McGraw Hill, New York, 1997.
 Huntley M, Redalje D. CO₂ mitigation and renewable oil from photosynthetic microbes: a new appraisal. *Mitigation Adapt Strat Global Change* 2007; 12:573-608.
 Jairaj KS, Singh SP, Srikant K. A review of solar dryers developed for grape drying. *Solar Energy* 2009; 83:1698-1712.
 Khoo HH, Sharratt PN, Das P, Balasubramanian RK, Naraharisetti PK, Shaik S. Life cycle energy and CO₂ analysis of microalgae-to-biodiesel: Preliminary results and comparisons. *Bioresource Technology* 2011; 102:5800-5807.
 Knothe G, Van Gerpen J, Krahl J. *The Biodiesel Handbook*. American Oil Chemists' Society Press, 2005.
 Koua KB, Fassinou WF, Gbaha P, Toure S. Mathematical modelling of the thin layer solar drying of banana, thin layer solar drying of banana, mango and cassava. *Energy* 2009; 34:1594-1602.
 Lahsasni S, Kouhila M, Mahrouz M, Idlimam A, Jamali A. Thin

- layer convective solar drying and mathematical modeling of prickly pear peel (*Opuntia ficus indica*). *Energy* 2004; 29:211-224.
- Mahmutoglu T, Emir F, Saygi YB. Sun/solar drying of differently treated grapes and storage stability of dried grapes. *Journal of Food Engineering* 1996; 29:289-300.
- Maloney JO. Perry's Chemical Engineers' Handbook, 8th Edition. McGraw Hill, New York, USA, 2008.
- Midilli A, Kucuk H. Mathematical modelling of thin layer drying of pistachio by using solar energy. *Energy Conversion and Management* 2003; 44(7):1111-1122.
- Montgomery DC, Runger GC. Applied statistics and probability for engineers, Third Edition. John Wiley & Sons, Inc., 2003.
- Patil V, Tran K-Q, Giselrød HR. Towards Sustainable Production of Biofuels from Microalgae. *International Journal of Molecular Sciences* 2008; 9:1188-1195.
- Prakash J, Pushparaj B, Carlozzi P, Torzillo G, Montaini E, Materassi R. Microalgae biomass drying by a simple solar device. *International Journal of Solar Energy* 1997; 18:303-311.
- Senate of the Philippines (SP). "Angara Supports Creation of Algae R&D HUB". Press Release. Accessed on July 10, 2013 [http://www.senate.gov.ph/press_release/2011/0527_angara2.asp]
- Show KY, Lee DJ, Chang JS. Algal biomass dehydration. *Bioresource Technology* 2013; 135:720-729.
- Simate I. Optimization of mixed-mode and indirect-mode natural convection solar dryers. *Renewable Energy* 2003; 28:435-453.
- Togrul IT, Pehlivan D. Mathematical modelling of solar drying of apricots in thin layers. *Journal of Food Engineering* 2002; 55:209-216.
- Usub T, Lertsatitthankorn C, Poomsa-Ad N, Wiset L, Siriamornpun S, Soponronnarit S. Thin layer solar drying characteristics of silkworm pupae. *Food and Bioprocess Processing* 2010; 88(2-3):149-160.
- Viswanathan T, Mani S, Das KC, Chinnasamy S, Bhatnagar A.. Drying characteristics of a microalgae consortium developed for biofuels production. *American Society of Agricultural and Biological Engineers* 2011; 54(6):2245-2252.
- Weller CL, Bunn JM. Drying rate constants for yellow dent corn as affected by fatty acid ester treatments. *American Society of Agriculture Engineers* 1993; 36(6):1815-1819.
- Yaldiz O, Ertekin C, Uzun HB. Mathematical modeling of thin layer solar drying of sultana grapes. *Energy* 2001; 26:457-465.